Available online at www.sciencedirect.com
SCIENCE DIRECT®
Optics Communications 241 (2004) 513–520
OPTICS COMMUNICATIONS
www.elsevier.com/locate/optcom

Z-scan formula for two-level atoms

Yingxue Wang, M. Saffman *

Department of Physics, University of Wisconsin-Madison, 1150 University Avenue, Madison, WI 53706, USA

Received 11 June 2004; received in revised form 13 July 2004; accepted 13 July 2004

Abstract

An analytical expression for the Z-scan signal from two-level atoms which show a saturable dispersive and absorptive nonlinearity is derived. An approximate solution is obtained for the normalized transmittance and compared with numerical calculations.

Keywords: Z-scan; Kerr media

1. Introduction

The Z-scan technique was originally developed in 1989 to measure nonlinear refraction in optical media [1,2] and has since been used widely for characterizing many different materials [3–12]. In Z-scan measurements the transverse profile of a laser beam passing through a nonlinear sample is investigated. In the presence of self-focusing or self-defocusing the transmittance of the beam through a small aperture placed after the sample yields a dispersion-shaped curve as a function of the sample position relative to the focal plane of the probe beam. The sign and magnitude of the nonlinear refractive index can be deduced from the transmittance curve. In many optical media, including polymers, photorefractive crystals, and atomic vapors, both the nonlinear absorption and nonlinear dispersion exhibit significant saturation effects at low optical intensity.

To explain the Z-scan transmittance curve theoretical calculations have been made by many authors [2,5,7,8,10,13–19]. Most studies have considered nonsaturable Kerr media with or without nonlinear absorption. A Gaussian decomposition (GD) method has been successfully used for thin samples [2,10,19]. Besides Yao et al. [17] introduced a diffraction model for thin sample. Various methods including an integral transformation [14], Hankel transformation [7], numerical fitting [8], variational analysis [16], and GD combined with

* Corresponding author. Tel.: +1 608 265 5601; fax: +1 608 265 2334.
E-mail address: msaffman@wisc.edu (M. Saffman).

0030-4018/$ - see front matter
doi:10.1016/j.optcom.2004.07.029

a distributed lens model [18], were used to calculate the Z-scan transmittance for thick media.

Previous work on Z-scan measurements in hot atomic vapors [9,11,12], used laser frequencies from a few hundred MHz to a few GHz away from the resonance so that the saturation effect was small. With the aid of laser cooling and trapping, the Doppler linewidth of the atoms can be reduced to the order of the natural linewidth or less so that a much smaller laser frequency detuning of order tens of MHz can be used. Experimental Z-scan measurements in this limit of small detuning [20,21] are influenced by saturation of both the dispersion and absorption. Bian et al. [13] studied the saturable Kerr nonlinearity analytically, but did not include the effects of nonlinear absorption which are important near resonance in atomic vapors. Oliveira et al. [5] studied numerically the saturable nonlinearity and accounted for the effect of saturable absorption in an approximate manner. In this paper, we study the nonlinearity of a near-resonant two-level atom by extending existing theories for saturable Kerr media to the case of general saturable dispersive and absorptive nonlinearity. The theoretical analysis is given in Section 2, and the results are compared with numerical calculations relevant to propagation in cold atomic vapors in Section 3.

2. Theory

Considering the geometry given in Fig. 1, we describe a sample with saturable Kerr nonlinearity and saturable absorption as follows:

$$\Delta n(I) = \frac{n_2 I}{1 + I/I_{s\Delta}}, \tag{1}$$

$$\alpha(I) = \frac{\alpha_0}{1 + I/I_{s\Delta}}, \tag{2}$$

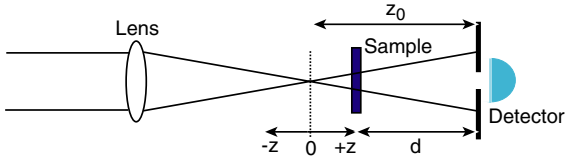

Fig. 1. Schematic diagram of Z-scan setup.

where n_2 is the nonlinear coefficient of refractive index, α_0 is the linear absorption coefficient, I is the laser beam intensity, and $I_{s\Delta}$ is the saturation intensity of the nonlinear material. If the beam intensity is small so $I < I_{s\Delta}$, we can expand the factor $(1 + I/I_{s\Delta})^{-1}$ in Eqs. (1) and (2)

$$\frac{1}{1 + I/I_{s\Delta}} = 1 - \frac{I}{I_{s\Delta}} + \frac{I}{I_{s\Delta^2}^2} + \cdots \tag{3}$$

Keeping the lowest two orders we have

$$\Delta n(I) \simeq n_2 I\left(1 - \frac{I}{I_{s\Delta}}\right), \tag{4}$$

$$\alpha(I) \simeq \alpha_0\left(1 - \frac{I}{I_{s\Delta}}\right). \tag{5}$$

For a TEM_{00} Gaussian beam with beam waist w_0, the complex field amplitude is

$$E(z,r) = E_p \frac{w_0}{w(z)} \exp\left\{-\frac{r^2}{w^2(z)} + \frac{ik_0 r^2}{2R(z)} - i\varphi(z)\right\}, \tag{6}$$

where E_p denotes the electric field at the focus, $w^2(z) = w_0^2(1 + z^2/z_R^2)$ and $R(z) = z(1 + z_R^2/z^2)$ are the beam radius and the radius of curvature at z, respectively, $z_R = k_0 w_0^2/2$ is Rayleigh range of the beam, $k_0 = 2\pi/\lambda$ is the wave number, λ is the wavelength in vacuum, and $\varphi(z,t) = \arctan(z/z_R)$ is the Guoy phase. What we are interested in here is the radial phase variation, the slowly varying envelope approximation applies and all other phase changes that are uniform in r are ignored. In the thin-sample limit, the sample thickness is small enough so that changes in the beam diameter within the sample due to either diffraction and nonlinear refraction can be neglected [1,2]. Define n_0 as the linear refractive index of the medium, the evolution of intensity $I = n_0\epsilon_0 c|E|^2/2$ and phase ϕ of the electric field as a function of z' (coordinate inside the nonlinear sample) are described by a pair of simple equations:

$$\frac{dI}{dz'} = -\alpha(I)I, \tag{7}$$

$$\frac{d\Delta\phi}{dz'} = \Delta n(I)k_0. \tag{8}$$

Substituting Eqs. (4) and (5) into Eqs. (7) and (8), and solving for I and $\Delta\phi$, we get at the exit surface of the nonlinear sample

$$I_e(z,r) = \frac{I(z,r)e^{-\alpha_0 L}}{1+Q(z,r)}, \tag{9}$$

$$\Delta\phi(z,r) = \Delta\phi_0(z)\left(1+\frac{Q(z,r)}{\alpha_0 L_{\text{eff}}}\right)\frac{e^{-2r^2/w^2(z)}}{1+Q(z,r)}, \tag{10}$$

where L is the nonlinear sample length,

$L_{\text{eff}} = (1-e^{-\alpha_0 L})/\alpha_0$,
$Q(z,r) = -\alpha_0 L_{\text{eff}} I(z,r)/I_{s\Delta}$,
$\Delta\phi_0(z) = \Delta\phi_0/(1+z^2/z_R^2)$,
$\Delta\phi_0 = n_2 k_0 I_p L_{\text{eff}}$, and
$I_p = 2P/(\pi w_0^2)$

is the peak beam intensity.

The complex electric field amplitude exiting the nonlinear sample including the nonlinear phase distortion is now

$$E_e(z,r) = \frac{E(z,r)e^{-\alpha_0 L/2}}{\sqrt{1+Q(z,r)}}e^{i\Delta\phi}. \tag{11}$$

By expanding the exponential function of the phase perturbation $\exp[i\Delta\phi]$

$$e^{i\Delta\phi(z,r)} = \sum_{m=0}^{\infty}\frac{[i\Delta\phi_0(z)]^m}{m!}\left[\left(1+\frac{Q}{\alpha_0 L_{\text{eff}}}\right)\left(\frac{e^{-2r^2/w^2(z)}}{1+Q}\right)\right]^m, \tag{12}$$

we can write the field Equation (11) as

$$E_e(z,r) = E(z,r)e^{-\alpha_0 L/2}\sum_{m=0}^{\infty}\frac{[i\Delta\phi_0(z)]^m}{m!} \times\left(1+\frac{Q}{\alpha_0 L_{\text{eff}}}\right)^m\frac{e^{-2mr^2/w^2(z)}}{(1+Q)^{m+1/2}}. \tag{13}$$

We then use,

$$\left(1+\frac{Q}{\alpha_0 L_{\text{eff}}}\right)^m\frac{1}{(1+Q)^{m+1/2}} = \left(1-\frac{I}{I_{s\Delta}}\right)^m\left(1-\alpha_0 L_{\text{eff}}\frac{I}{I_{s\Delta}}\right)^{-m-1/2} = \sum_{n=0}^{m}\sum_{p=0}^{\infty}(-1)^n\frac{m!(m+\frac{1}{2})_p}{(m-n)!n!p!} \times(\alpha_0 L_{\text{eff}})^p\left(1-\frac{I}{I_{s\Delta}}\right)^{(n+p)}, \tag{14}$$

where $(m+\frac{1}{2})_p = (m+\frac{1}{2})(m+\frac{3}{2})\cdots(m+p-\frac{1}{2})$ is a Pochhammer symbol [22]. Following the GD method used by Weaire et al. [23], we can write down the electric field amplitude at the aperture as

$$E_a(r) = E(z,0)e^{-\alpha_0 L/2} \times\sum_{m,p=0}^{\infty}\sum_{n=0}^{m}\frac{(-1)^n(m+\frac{1}{2})_p}{(m-n)!n!p!}[i\Delta\phi_0(z)]^m \times\frac{(\alpha_0 L_{\text{eff}})^p s^{n+p}}{(1+z^2/z_R^2)^{n+p}}\frac{w_{mnp0}}{w_{mnp}} \times\exp\left\{-\frac{r^2}{w_{mnp}^2}+\frac{ik_0 r^2}{2R_{mnp}}-i\theta_{mnp}\right\}. \tag{15}$$

We define $s = I_p/I_{s\Delta}$ as the on-axis saturation parameter, d as the propagation distance in free space from the nonlinear sample to the aperture plane and $g = 1 + d/R(z)$, the other parameters are

$$w_{mnp0}^2 = \frac{w^2(z)}{2(m+n+p)+1},$$
$$w_{mnp}^2 = w_{mnp0}^2\left(g^2+\frac{d^2}{d_{mnp}^2}\right),$$
$$d_{mnp} = \frac{1}{2}k_0 w_{mnp0}^2, \tag{16}$$
$$R_{mnp} = d\left(1-\frac{g}{g^2+d^2/d_{mnp}^2}\right)^{-1},$$
$$\theta_{mnp} = \arctan\frac{d/d_{mnp}}{g}.$$

From Eq. (15), the transmittance of the aperture is calculated as

$$T(z) = \frac{\int_0^{r_a}|E_a(r)|^2 r\,dr}{\int_0^{r_a}|E(z_0,r)|^2 r\,dr}, \tag{17}$$

where z_0 is the distance between the probe beam waist and the aperture.

The on-axis electric field at the aperture can be obtained by setting $r = 0$ in Eq. (15)

$$E_a(0) = E(z,0)e^{-\alpha_0 L/2}[F_0 + i\Delta\phi_0(z)F_1 - \Delta\phi_0^2(z)F_2 + \sigma], \tag{18}$$

where σ is the summation of terms proportional to $(\Delta\phi_0)^m$ with $m \geqslant 3$ and

$$F_m = \sum_{n=0}^{m}\sum_{p=0}^{\infty} \frac{(-1)^n (m+\frac{1}{2})_p}{(m-n)!n!p!} \frac{(\alpha_0 L_{\mathrm{eff}})^p s^{n+p}}{(1+z^2/z_R^2)^{n+p}} \frac{1}{g+\mathrm{i}\frac{d}{d_{mnp}}}.$$

Substituting g, d_{mnp} and $x = z/z_R$ into F_m above we get

$$F_m = \sum_{n=0}^{m}\sum_{p=0}^{\infty} \frac{(-1)^n (m+\frac{1}{2})_p}{(m-n)!n!p!} \left(\frac{z_R}{d}\right) \times \frac{(\alpha_0 L_{\mathrm{eff}})^p s^{n+p}}{(x^2+1)^{n+p-1}[z_R(x^2+1)/d + x + \mathrm{i}(2(m+n+p)+1)]}. \tag{19}$$

From Eqs. (18) and (19), the on-axis transmittance ignoring σ is

$$T(z) = \frac{|E_a(0)|^2}{|E(z_0,0)|^2} = \frac{z_0^2/z_R^2+1}{x^2+1} \mathrm{e}^{-\alpha_0 L} |F_0|^2 \left| 1 + \mathrm{i}\Delta\phi_0(z)\frac{F_1}{F_0} - \Delta\phi_0^2(z)\frac{F_2}{F_0}\right|^2. \tag{20}$$

The Z-scan transmittance [20] depends on the terms F_1,F_2, and F_3 which are due to both the nonlinear dispersion and absorption. If the beam intensity is very low so that we only keep the term proportional to s in Eq. (19),

$$F_0 = \left(\frac{z_R}{d}\right)\left[\frac{x^2+1}{z_R(x^2+1)/d + x + \mathrm{i}} + \frac{\alpha_0 L_{\mathrm{eff}}}{2}\frac{s}{z_R(x^2+1)/d + x + 3\mathrm{i}}\right],$$

$$F_1 = \left(\frac{z_R}{d}\right)\left[\frac{x^2+1}{z_R(x^2+1)/d + x + 3\mathrm{i}} + \left(\frac{3}{2}\alpha_0 L_{\mathrm{eff}} - 1\right)\frac{s}{z_R(x^2+1)/d + x + 5\mathrm{i}}\right],$$

$$F_2 = \left(\frac{z_R}{d}\right)\left[\frac{x^2+1}{2(z_R(x^2+1)/d + x + 5\mathrm{i})} + \left(\frac{5}{4}\alpha_0 L_{\mathrm{eff}} - 1\right)\frac{s}{z_R(x^2+1)/d + x + 7\mathrm{i}}\right],$$

In the far field $z_R \ll d$ and $z_0 \approx d$, so the on-axis transmittance simplifies to

$$T(z) = \mathrm{e}^{-\alpha_0 L}[T_{\mathrm{k}}(z) + T_{\mathrm{s}}(z) + T_{\mathrm{c}}(z)], \tag{21}$$

with

$$T_{\mathrm{k}}(z) = 1 + \frac{4\Delta\phi_0 x}{(x^2+1)(x^2+9)} + \frac{4\Delta\phi_0^2(3x^2-5)}{(x^2+1)^2(x^2+9)(x^2+25)}, \tag{22}$$

$$T_{\mathrm{s}}(z) = -\frac{8\Delta\phi_0 s x}{(x^2+1)^2(x^2+25)} - 2\Delta\phi_0^2 s\left[\frac{(x^2+15)}{(x^2+1)^2(x^2+9)(x^2+25)} - \frac{x^2+7}{(x^2+1)^3(x^2+49)}\right], \tag{23}$$

$$T_{\mathrm{c}}(z) = \frac{\Delta\psi_0(x^2+3)}{(x^2+1)(x^2+9)} + \frac{12\Delta\phi_0\Delta\psi_0 x}{(x^2+1)^2(x^2+25)} + \frac{5\Delta\phi_0^2\Delta\psi_0}{2}\left[\frac{(x^2+15)}{(x^2+1)^2(x^2+9)(x^2+25)} - \frac{(x^2+7)}{(x^2+1)^3(x^2+49)}\right] \tag{24}$$

where $\Delta\psi_0 = \alpha_0 L_{\mathrm{eff}} s$, $T_{\mathrm{k}}(z)$ is the Z-scan transmittance for Kerr media [2,13], $T_{\mathrm{s}}(z)$ is the correction due to the saturable nonlinearity [13], and $T_{\mathrm{c}}(z)$ includes the coupled effect of nonlinear absorption and saturable nonlinearity.

3. Discussion

We will compare the above analytical results with numerical calculations for the specific case of a cloud of two-level atoms. We assume a scalar electric field $\varepsilon = [E(\mathbf{r}, z)/2]\mathrm{e}^{\mathrm{i}(kz-\omega t)} + [E^*(\mathbf{r}, z)/2]\mathrm{e}^{-\mathrm{i}(kz-\omega t)}$, the paraxial wave equation describing the propagation of the field amplitude in two-level atoms is [24]

$$\frac{\partial E}{\partial z} - \frac{\mathrm{i}}{2k}\nabla_{\perp}^2 E = \mathrm{i}\frac{3\lambda^2}{4\pi n_0} n_{\mathrm{a}} W_0 \frac{2\Delta/\gamma - \mathrm{i}}{1 + 4\Delta^2/\gamma^2 + I/I_{\mathrm{s}}} E, \tag{25}$$

from which the nonlinear susceptibility is derived as

$$\chi = \frac{3\lambda^3 n_{\mathrm{a}} W_0}{4\pi^2}\frac{2\Delta/\gamma - \mathrm{i}}{1 + 4\Delta^2/\gamma^2 + I/I_{\mathrm{s}}}. \tag{26}$$

Here n_a is the number density of atoms, W_0 is the population difference in thermal equilibrium, generally $W_0 = -1$, λ is the wavelength of the laser beam in vacuum, $k = n_0 k_0 = n_0 2\pi/\lambda$ is the wave number in the medium, γ is the decay rate of the excited state, Δ is the laser beam detuning with respect to the transition frequency, I_s is the on resonance saturation intensity of atoms and I is the actual field intensity. The nonlinear susceptibility χ in Eq. (26) shows saturation behavior in both refractive index (Re[χ]) and absorption coefficient (Im[χ]). Defining the saturation intensity with arbitrary detuning $I_{s\Delta} = I_s(1 + 4\Delta^2/\gamma^2)$, for $I < I_{s\Delta}$ and small absorption, we get the same relation for nonlinear refractive index and absorption coefficient as Eqs. (1) and (2), where the linear refractive index, nonlinear coefficient of refractive index and absorption coefficient are

$$n_0 = 1 + \frac{3\lambda^3 n_a W_0}{4\pi^2} \frac{\Delta/\gamma}{1 + 4\Delta^2/\gamma^2} \simeq 1, \tag{27}$$

$$n_2 = -\frac{3\lambda^3}{4\pi^2 n_0} \frac{n_a W_0}{I_{s\Delta}} \frac{\Delta/\gamma}{1 + 4\Delta^2/\gamma^2}, \tag{28}$$

$$\alpha_0 = \frac{3\lambda^3 n_a}{2\pi} \frac{1}{1 + 4\Delta^2/\gamma^2}. \tag{29}$$

From Eq. (28), the nonlinear response of two-level atoms to a near-resonance optical field can be self-defocusing or self-focusing for different laser detunings. If the laser frequency is tuned to the red side of the resonance, i.e., $\Delta < 0$, then $n_2 < 0$, the laser beam is self-defocused by atoms. On the contrary, the beam is self-focused by atoms if its frequency is blue-detuned, i.e., $\Delta > 0$. In the following, we numerically solve the wave equation (25) on a 128×128 point transverse grid using a split-step method to get the on-axis transmittance, and then compare the results with analytical ones calculated from Eq. (20) for both self-defocusing and self-focusing.

3.1. Low beam intensity $s \ll 1$

For a thin sample when beam the intensity is very low such that $s \ll 1$, only terms with $m = n = p = 0$ in Eq. (20) are important and the transmittance can be obtained from Eq. (22), which is exactly the on-axis transmittance for nonsaturable Kerr media without nonlinear absorption [2,13].

3.2. Moderate beam intensity close to the resonance $s < 1$

We have chosen uniformly distributed cesium atoms as the nonlinear medium with the following parameters: length of the medium $L = 0.6$ mm, atomic density $n_a = 8.0 \times 10^{10}$ cm^{-3}, laser beam wavelength $\lambda = 852.1$ nm, Gaussian waist of the beam $w_0 = 30.0$ μm. The frequency of the laser beam is detuned from the center of the $F = 4 \rightarrow F' = 5$ transition of the D2 line by $\Delta = \pm 4\gamma$, and the saturation intensity is $I_{s\Delta} = 71.5$ mW/cm^2. The beam peak intensity is 28.3 mW/cm^2 such that $s = 0.4$ and $\Delta\phi_0 = 0.4$. The aperture is placed $z_0 = 2.5$ cm away from the beam waist. The transmittance from Eq. (20) is shown in Figs. 2 and 3.

Both figures show that the analytical results converge as more terms from the summation in F_m are included into the calculation in Eq. (20). Compared with the numerical results shown by the solid line in figures, when only one term is used in each F_m so that $p_{max} = 0$, the analytical results have a similar shape but are overall lower. When more than one term ($p_{max} \geqslant 1$) is used in each F_m, the analytical results converge quickly and agree with the numerical results.

In Eq. (20), we took only the first three terms in the summation over m and dropped those propor-

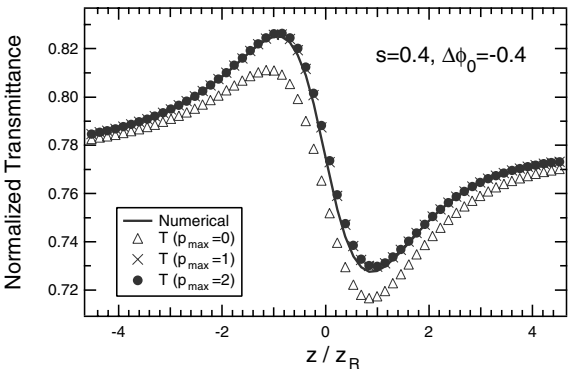

Fig. 2. Analytical transmittance retaining the 1st, 2nd and 3rd terms in F_m ($p_{max} = 0$, 1, 2) compared with the numerical calculation for self-defocusing.

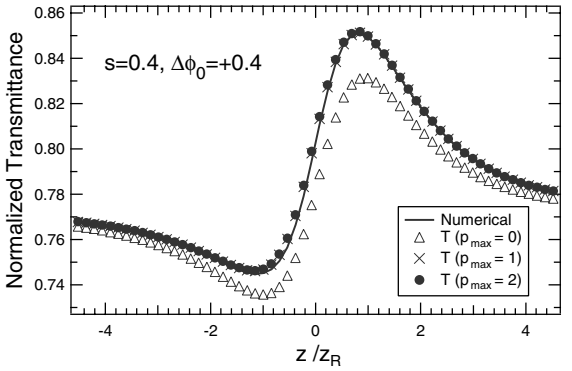

Fig. 3. Analytical transmittance compared with the numerical calculation for self-focusing.

tional to $(\Delta\phi_0)^3$ and higher. We can estimate the error introduced by dropping the 4th term in Eq. (18),

$$\begin{aligned}\sigma &\leqslant |\Delta\phi_0(z)|^3 \left| \sum_{n=0}^{3} \sum_{p=0}^{\infty} \frac{(-1)^n (\frac{7}{2})_p}{(3-n)!n!p!} \right. \\ &\quad \left. \times \frac{(\alpha_0 L_{\mathrm{eff}})^p s^{p+n}}{(1+z^2/z_R^2)^{p+n}} \frac{1}{g+\mathrm{i}d/d_{3np}} \right| \\ &\leqslant 4|\Delta\phi_0(z)|^3 \left| \sum_{p=0}^{\infty} \frac{(\frac{7}{2})_p}{6p!} \frac{(\alpha_0 L_{\mathrm{eff}} s)^p}{(1+z^2/z_R^2)^p} \frac{1}{g+\mathrm{i}d/d_{3np}} \right| \\ &= \frac{2}{3} \frac{|\Delta\phi_0(z)|^3}{\sqrt{g^2+d^2/d_{300}^2}} \left(1 - \frac{\alpha_0 L_{\mathrm{eff}} s}{(z^2/z_R^2+1)}\right)^{-\frac{7}{2}} \end{aligned} \tag{30}$$

As the sample is moved away from the beam waist, σ drops rapidly. At $z = 0$, $d = z_0$ and $g = 1$, using the parameters above we have $\sigma \approx 1.1 \times 10^{-3}$, and $|\sigma/F_0| \approx 10^{-2}$. So the relative error in transmittance introduced by dropping the 4th term is 1%. From Figs. 2 and 3, the maximum relative error between the numerical calculation and Eq. (20) is about 1%. Thus, Eq. (30) gives a reasonable estimation of the error.

3.3. Nonlinear absorption and saturable nonlinearity

As we mentioned above, Eq. (20) includes the coupled nonlinear absorption and saturable nonlinearity. We check the effect of nonlinear absorption by setting the laser beam peak intensity to be 14.1 mW/cm^2 and changing its frequency detuning from $\Delta = +2\gamma$ to $\Delta = +10\gamma$ so as to change s and $\Delta\phi_0$. The other parameters are the same as in subsection 3.2. The Z-scan transmittance is shown in Fig. 4. When the laser frequency is tuned close to the resonance, near the beam waist the absorption is strongly saturated and the transmittance is increased. So the nonlinear absorption greatly enhances the transmittance peak and suppresses its valley. When the laser frequency is far away from the resonance, the nonlinear aborption is weak and the Z-scan transmittance curve returns to the normal dispersive shape.

When comparing the analytical calculations with the numerical results in Fig. 4, we see that the agreement is not perfect as s increases. We now calculate the Z-scan transmittance for different beam intensities with frequency detuning of $\Delta = +4\gamma$, the other parameters are the same as subsection 3.2. As shown in Fig. 5 the difference between the analytical and the numerical results increases as s increases. The disagreement between analytics and numerics is at the level of a few percent when $s \leqslant 1$. For example, at $s = 1$, the analytical transmittance is higher than the numerical value by only 5.5% at $z/z_R = 0.23$ and the peak to valley difference ΔT_{pv}, which is a measurement of nonlinear refractive index, is 7% smaller than that from the numerical results. For all calculations from Eq. (20) in Fig. 5, we have chosen $p_{\max} = 2$.

In order to compare closely with the numerics, we included more terms from Eq. (15) to calculate

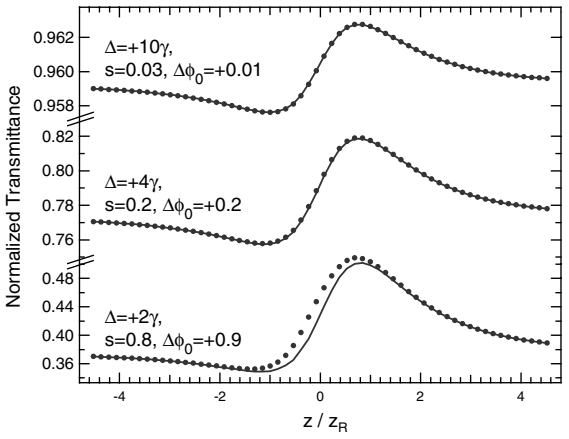

Fig. 4. Analytical transmittance (dots, $p_{\max} = 2$) compared with the numerical calculation (lines) for self-focusing with different frequency detunings.

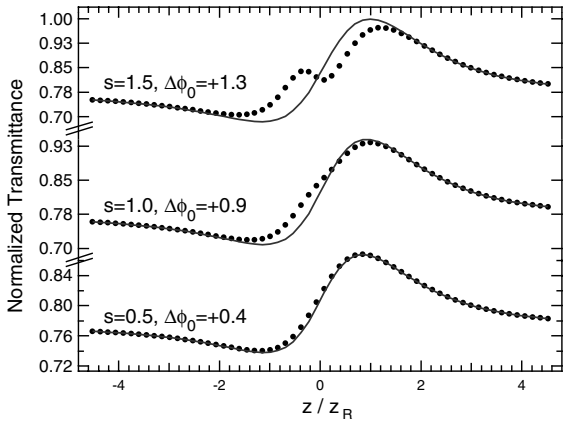

Fig. 5. Analytical transmittance (dots, $p_{max} = 2$) compared with the numerical calculation (lines) for self-focusing with different saturation paramters s.

the on-axis transmittance T, and the results were the same. So the difference between the analytical calculations and the numerics is not due to the inadequate number of terms in the summation but due to the approximation we have made in Eqs. (4) and (5). In both equations, we replace the saturation effect $1/(1 + I/I_{s\Delta})$ by $(1 - I/Is_{\Delta})$. For small $s = I/Is_{\Delta}$, it is a good approximation, when s increases, the nonlinear response shows strong saturation effects, and we would need to include more terms in the expansion Equation (3). When s increases further such that $s > 1$, approximations (4) and (5) are not valid any more, and the analytical results show a big difference with the numerical ones. Other approaches are needed to calculate the transmittance in this regime.

To further check the saturation effect, we fix the beam intensity to be 50.0 mW/cm^2 so that $s = 0.7$ and $\Delta\phi_0 = 0.6$, keep other parameters the same as in Fig. 5, and compare different analytical calculations with the numerical result in Fig. 6. The analytical calculations include the transmittance for simple Kerr media [2], saturable Kerr media without nonlinear absorption [13], nonsaturable Kerr media with nonlinear absorption [2,7], and the transmittance from Eq. (20) which includes both saturable nonlinearity and absorption. It is clear from the figure that our result using Eq. (20) agrees best with the numerical calculations. It shows that the transmittance peak has been enhanced and valley has been suppressed because of the nonlinear absorption and ΔT_{pv} is 16% smaller than that from nonsaturable Kerr media [2]. Among other analytical results, although Bian et al. [13] showed smaller ΔT_{pv} due to the saturation, the transmittance is a dispersive curve with peak and valley the same distance away from the horizontal level without nonlinear absorption [2,13]. When only the nonlinear absorption is included [7], the calculation agrees better with the numerics than those without nonlinear absorption, but it shows larger ΔT_{pv} than that from the numerics, which is due to the absence of saturation of the nonlinearity (Fig. 6).

3.4. Thick sample ($L/z_R \sim 1$)

We also calculated the transmittance for different sample thicknesses using Eq. (20) and compared them with the numerical solutions in Fig. 7. Although the Gaussian decomposition method is valid only when the sample is thin enough to ignore the diffraction inside the sample, the analytical results from Fig. 7 agree very well with the numerics even when L is close to z_R. At $L = z_R$, ΔT_{pv} from the analytics is only 2% higher than that from the numerics. When the sample is thicker than the Rayleigh range of the beam, the analytical result shows that the peak and valley transmittance are still at the same distance relative to focus and $\Delta T_{pv} = 0.078$. On the other hand the numerics show that this symmetry no longer holds due to the larger

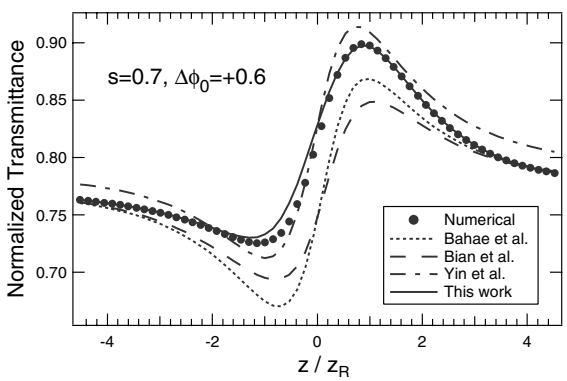

Fig. 6. Z-scan transmittance for Kerr media [2], saturable Kerr media [13], Kerr meida with nonlinear absorption [2,7] saturable Kerr media with nonlinear absorption (this work).

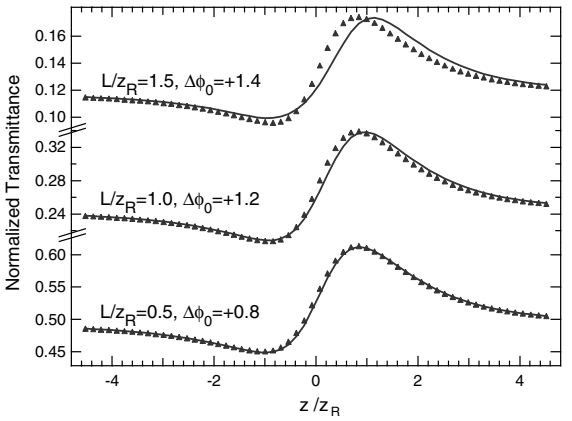

Fig. 7. Analytical transmittance (symbols, $p_{\max} = 2$) compared with the numerical calculations (lines) for self-defocusing with different sample lengths.

phase distortion $\Delta\phi_0 > 1$ and $\Delta T_{pv} = 0.074$. When $L > z_R$, the diffraction can no longer be ignored so a "thin sample" approximation is inaccurate in predicting the exact shape of the transmittance curve.

4. Conclusion

We have derived an analytical expression for the Z-scan transmittance of a nonlinear medium with saturable absorption and dispersion. Comparison with numerical solutions shows that our analytical result Eq. (20) is accurate up to saturation values of order unity. Eq. (20) is also more accurate than previously published expressions in the presence of saturable absorption. Although we started with the "thin sample" approximation $L/z_R \ll 1$ and low beam intensity $s < 1$, analytical calculations agree reasonably with numerics even when $s \sim 1$ and $L/z_R \sim 1$.

Acknowledgements

Support was provided by The University of Wisconsin Graduate School, and NSF Grant PHY-0210357.

References

[1] M. Sheik-Bahae, A.A. Said, E.W.V. Stryland, Opt. Lett. 14 (1989) 955.
[2] M. Sheik-Bahae, A.A. Said, T.-H. Wei, D.J. Hagan, E.W.V. Stryland, IEEE J. Quantum Electron. 26 (1990) 760.
[3] L. Yang, R. Dorsinville, Q.Z. Wang, P.X. Ye, R.R. Alfano, Opt. Lett. 17 (1992) 323.
[4] P.B. Chapple, J. Staromlynska, R.G. McDuff, J. Opt. Soc. Am. B 11 (1994) 975.
[5] L.C. Oliveira, T. Catunda, S.C. Zilio, Jpn. J. Appl. Phys., Part 1 35 (1996) 2649.
[6] R. Ryf, A. Lötscher, C. Bosshard, M. Zgonik, P. Günter, J. Opt. Soc. Am. B 15 (1998) 989.
[7] M. Yin, H.P. Li, S.H. Tang, W. Ji, Appl. Phys. B 70 (2000) 587.
[8] T. Hashimoto, T.Y. adn Tomohiro Kato, H. Nasu, K. Kamiya, J. Appl. Phys. 90 (2001) 533.
[9] S. Sinha, G.K. Bhowmick, S. Kundu, S. Sasikumar, S.K.S. Nair, T.B. Pal, A.K. Ray, K. Dasgupta, Opt. Commun. 203 (2002) 427.
[10] G. Tsigaridas, M. Fakis, I. Polyzos, M. Tsibouri, P. Persephonis, V. Giannetas, J. Opt. Soc. Am. B 20 (2003) 670.
[11] C.F. McCormick, D.R. Solli, R.Y. Chiao, J.M. Hickmann, J. Opt. Soc. Am. B 20 (2003) 2480.
[12] C.F. McCormick, D.R. Solli, R.Y. Chiao, J.M. Hickmann, Phys. Rev. A 69 (2004) 023804.
[13] S. Bian, M. Martinelli, R.J. Horowicz, Opt. Commun. 172 (1999) 347.
[14] J.A. Hermann, R.G. McDuff, J. Opt. Soc. Am. B 10 (1993) 2056.
[15] X. Liu, S. Guo, H. Wang, L. Hou, Opt. Commun. 197 (2001) 431.
[16] W.-P. Zang, J.-G. Tian, Z.-B. Liu, W.-Y. Zhou, C.-P. Zhang, G.-Y. Zhang, Appl. Opt. 42 (2003) 2219.
[17] B. Yao, L. Ren, X. Hou, J. Opt. Soc. Am. B 20 (2003) 1290.
[18] W.-P. Zang, J.-G. Tian, Z.-B. Liu, W.-Y. Zhou, F. Song, C.-P. Zhang, J. Opt. Soc. Am. B 21 (2004) 63.
[19] W.-P. Zang, J.-G. Tian, Z.-B. Liu, W.-Y. Zhou, F. Song, C.-P. Zhang, J. jun Xu, J. Opt. Soc. Am. B 21 (2004) 349.
[20] G. Labeyrie, T. Ackemann, B. Klappauf, M. Pesch, G.L. Lippi, R. Kaiser, Eur. Phys. J. D 22 (2003) 473.
[21] Y. Wang, M. Saffman, Phys. Rev. A 70 (2004) 013801.
[22] M. Abramowitz, I.A. Stegun, Handbook of Mathematical Functions with Formulas, Graphs and Mathematical Tables, Dover, New York, 1972.
[23] D. Weaire, B.S. Wherrett, D.A.B. Miller, S.D. Smith, Opt. Lett. 4 (1979) 331.
[24] R.W. Boyd, Nonlinear Optics, second ed., Academic Press, San Diego, 2003.